Tunneling Spectroscopy of bcc (001) Surface States

Joseph A. Stroscio, D. T. Pierce, A. Davies, and R. J. Celotta
Electron Physics Group, National Institute of Standards and Technology, Gaithersburg, Maryland 20899

M. Weinert
Physics Department, Brookhaven National Laboratory, Upton, New York 11973
(Received 30 June 1995)

We have discovered an intense, sharp feature in tunneling spectra of the Fe(001) and Cr(001) surfaces that derives from a bcc surface state near the Fermi level. Band-structure calculations show that this state is a general feature of bcc (001) surfaces, and that it originates from a nearly unperturbed d orbital extending out into the vacuum region. This general feature should permit chemical identification with atomic spatial resolution on bcc (001) surfaces. The surface state is in the minority spin band for Fe and Cr, so it should be useful for future spin-polarized tunneling experiments.

PACS numbers: 61.16.Ch, 73.20.At

Since the realization of the scanning tunneling microscope (STM) [1], tunneling spectroscopy with the STM has offered the possibility of probing the energy dependence of the electron states in the sample and the tip, permitting examination of electronic states with spatial selectivity [2,3]. One potential benefit is the identification of different chemical species. To date the most numerous applications of scanning tunneling spectroscopy have been in the area of semiconductor surfaces, where different electronic states have been identified on various surface reconstructions [4]. In contrast, the application to metal surfaces has not been as widespread, partly because early tunneling spectra of metal surfaces were relatively featureless [5,6]. Recently, chemically selective imaging in metal systems has been achieved by utilizing tunneling into the barrier-resonance states, which vary in energy with the work function of the metal [7]. Chemical selectivity has also been seen intermittently in PtNi alloys, although the origin of that contrast is unknown [8].

By far, the largest features in STM spectra are expected to arise from surface states and resonances that result from broken translational symmetry along the surface normal, and whose wave functions have large amplitudes in the surface layers of a crystal. On the (111) noble metal surfaces of Au, Ag, and Cu there is a unique surface state lying in a partial band gap. This state has been observed in STM tunneling spectra, and displays a rich variety of spatial quantum interference patterns because of its two-dimensional free-electron character [9–11].

In this Letter, we present the tunneling spectra of Fe(001) and Cr(001) surfaces. We find that both of these surfaces display an intense, sharp peak in the tunneling spectra near the Fermi level (E_F). Based on a comparison with band-structure calculations of Fe(001) and Cr(001), we find that this sharp feature arises from a (minority band) surface state near the center of the surface Brillouin zone $\overline{\Gamma}$ that is a general feature of bcc (001) surfaces. Chemical identification with atomic spatial resolution should be possible utilizing these surface states because of their location near E_F. This contrasts to recent chemical imaging requiring high tunneling voltages into barrier-resonance states [7]. Such high voltages prevent atomic resolution measurements. In the case of a ferromagnetic material like Fe(001), this spin-polarized d-like state should also facilitate spin dependent tunneling experiments.

The experiments were performed on Fe(001) single crystal whisker surfaces in an ultrahigh vacuum system with pressures in the range of 3×10^{-9} Pa. The Fe whiskers are grown by high temperature decomposition of FeCl. Surfaces of these whiskers are of extremely high quality having terraces 1 μm wide or larger [12,13]. The Fe whisker surfaces are cleaned by ion sputtering at 750 °C. Clean surfaces show 1×1 atomic lattices in STM measurements. Cr(001) surfaces are prepared by growing epitaxial Cr films on the Fe(001) whiskers. STM measurements are made at room temperature with W(111) oriented tips prepared *in situ* by field electron and ion emission techniques.

Figure 1 shows the tunneling conductance spectra of the Fe(001) surface recorded at several tip-sample separations [Fig. 1, curves (a)–(f)]. All the spectra show a very narrow feature 0.17 eV above the Fe Fermi level, defined as 0 V. The strength of this feature increases as the tip-sample distance is reduced, as expected from the exponential distance dependence of tunneling matrix elements. Two noteworthy features of this conductance peak are its strength and narrow width. The strength of this feature is such that the additional tunneling channel opened by the conductance peak is sufficient to yield a very asymmetric current-voltage curve with approximately twice as much tunnel current at a sample bias of +1.0 V as compared to −1.0 V. The narrow feature width of 0.13 eV (FWHM) is comparable to the thermal broadening in the tunneling measurement ($\sim 5k_BT$). The inherent width of this feature may be much narrower.

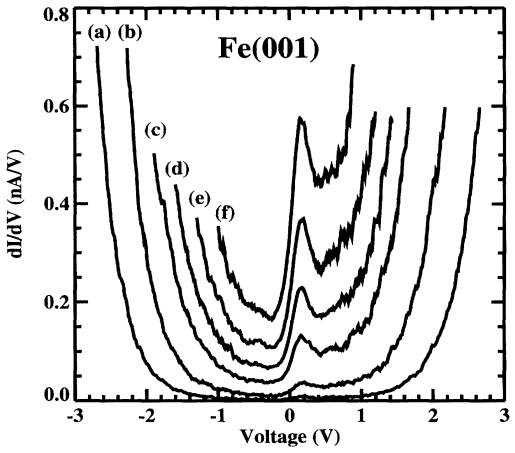

FIG. 1. Tunneling conductance vs sample voltage measurements of an Fe(001) surface obtained at constant height above the Fe surface. Curves (a)–(f) correspond to different tunneling distances between the tip and sample obtained by stabilizing the initial tunneling conditions with different initial sample voltages from (a) 3, (b) 2.5, (c) 2.0, (d) 1.7, (e) 1.4, and (f) 1.1 V. The tunneling conductance data were obtained from the numerical differentiation of the current vs voltage measurements using an energy window of 0.05 eV to calculate the local slope. The FWHM, 0.13 eV, and center position, 0.17 eV, of the conductance peak were determined by fitting the peak with a Gaussian function plus a quadratic background.

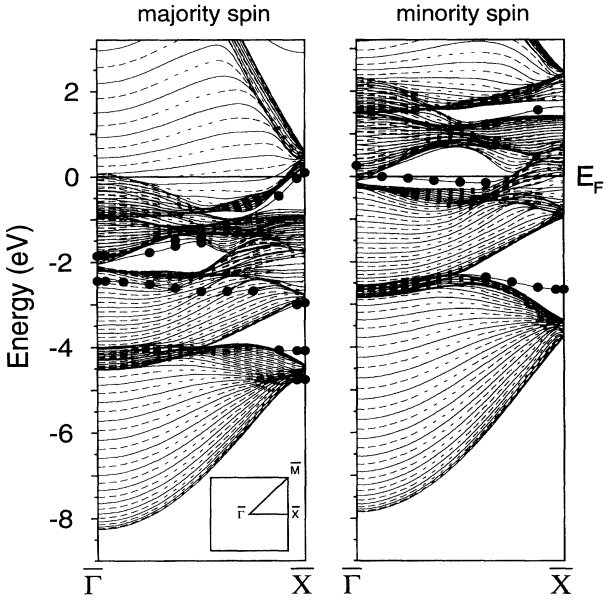

FIG. 2. Band structure of majority and minority even symmetry states along $\bar{\Gamma}$-$\bar{X}$ for a 49-layer Fe(001) film. States with high localization in the surface region are marked with circles.

Such a sharp feature is unusual in STM spectra on metal surfaces. The feature in Fig. 1 was reproducibly observed in measurements on multiple Fe(001) whiskers with numerous W(111) tips. The feature is derived from the Fe(001) substrate and not the tip; a feature at a different energy was observed for Cr(001), as discussed below. In order to identify the origin of the spectra in Fig. 1, we performed band-structure calculations of the Fe(001) surface using the full-potential linearized augmented plane wave (FLAPW) method.

The result of this calculation is shown in Fig. 2, where the band structure of the Fe(001) surface is illustrated along the $\bar{\Gamma}$-$\bar{X}$ direction for majority and minority electron spin. States with mainly surface amplitude are indicated by the solid circles. Surface states and resonances are observed throughout the $\bar{\Gamma}$-$\bar{X}$ direction. The minority resonance and surface state at -2.5 eV has previously been observed by spin-polarized–angle-resolved photoemission [14]. It is accurately predicted by these FLAPW calculations for majority and minority electron spins for a 49-layer film [15].

From Fig. 2, it is seen that there are surface states just above the Fermi level, which could give rise to the conductance peak observed in Fig. 1, at the $\bar{\Gamma}$ point for the minority states, and at the $\bar{X}$ point for the majority states. Moreover, there are additional surface states and resonances near the Fermi level at other points in the Brillouin zone. To determine which states contribute to the STM tunneling spectra, it is useful to examine the form of the tunneling current for a suitable model of the tip, such as a spherical geometry as described by Tersoff and Hamann [16]. The tunneling current is given by an energy integral over the local density of states of the sample, assuming a uniform tip density of states. The tunneling conductance measurements, which are the derivative of the tunneling current, are to first order at low bias voltages given by the local density of states (LDOS) at a position above the surface at the center of radius of the probe tip for a spherical probe tip geometry [16]. At such a distance (0.5 to 1 nm) the states at $\bar{\Gamma}$ will dominate the tunneling, as the wave functions in the vacuum region decay asymptotically as $\exp[(\kappa^2 + \mathbf{k}_{\|}^2)^{1/2} z]$, where κ is the minimum decay constant (around 11 nm^{-1}) and $\mathbf{k}_{\|}$ is the parallel wave vector. States at the center of the surface Brillouin zone ($\mathbf{k}_{\|} = 0$) decay most slowly, giving the largest tunneling probability. For comparison, the relative tunneling probability for states at the $\bar{X}$ point will be reduced by a factor 10^{-4} at 1 nm from the surface.

Figure 3 shows the majority, minority, and total LDOS around $\bar{\Gamma}$, integrated over $\mathbf{k}_{\|}$ in a circular region around $\bar{\Gamma}$, out to $\frac{1}{6}$ the distance from $\bar{\Gamma}$-$\bar{X}$. The LDOS are shown at various heights above the surface. The integrated LDOS are dominated by the structure at $\bar{\Gamma}$. Comparing to the tunneling spectra in Fig. 1, we observe excellent agreement with the surface state at 0.2 eV just above the Fermi level in the minority band [Fig. 3(b)]. This surface state results from a nearly unperturbed $d_{3z^2-r^2}$ orbital (z is normal to the surface), which has a large amplitude in the vacuum region outside the surface, as

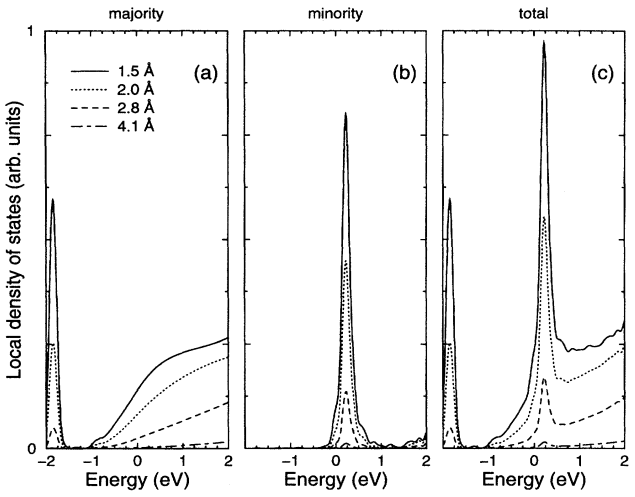

FIG. 3. Local density of states at various distances above the Fe(001) surface arising from states with $|\mathbf{k}_{\|}| < \frac{1}{6}|\overline{\Gamma}-\overline{X}|$ for (a) majority, (b) minority, and (c) both spins.

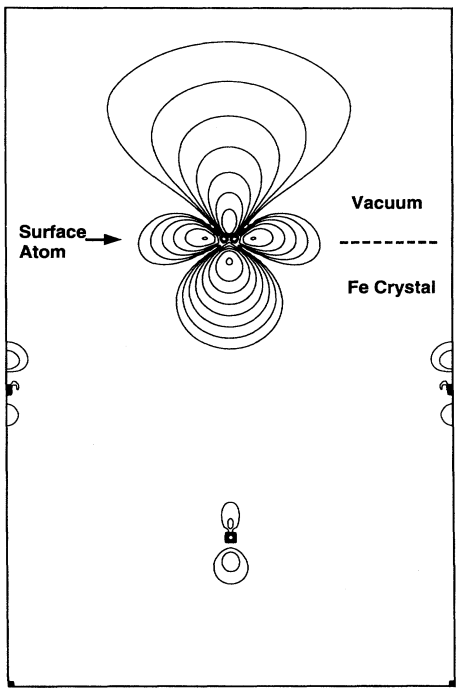

FIG. 4. Plot of the density from the minority surface state at $\overline{\Gamma}$ in a (110) plane through the Fe crystal. Adjacent contours differ by factors of 2, with the lowest contour at 34 electrons nm^{-3}.

shown in Fig. 4. The majority LDOS shows contributions above the Fermi level from the bulk Δ_1 states [the bulk Δ_1 states are completely symmetric with respect to the symmetry operations of a square (the group C_{4v}), e.g., s and $d_{3z^2-r^2}$ orbitals]. A sharp peak at -1.8 eV is also observed in Fig. 3(b), which is the exchange-split partner of the 0.2 eV minority state.

Since our measurements are not spin resolved, the appropriate comparison to the data in Fig. 1 is the total LDOS in Fig. 3(c). The additional feature at -1.8 eV in Fig. 3(c), originating from the majority band, is not seen in the tunneling spectrum in Fig. 1. This state is difficult to detect in the tunneling spectra because of its energy location below E_F. The relative tunneling probability of this state, compared to tunneling from states at the Fermi level, is reduced by a factor of 10^{-2} (at 1 nm above the surface) because of the faster decay into the vacuum of the majority state and the higher tunneling barrier seen by states 2 eV below the Fermi level.

Zone-center surface states near the Fermi level are found on a number of bcc (001) surfaces. Such surface states were first seen in field emission energy distributions from W(001) [17]. They also have been observed using angle-resolved photoemission on W(001) [18] and Ta(001) [19] and have been obtained in calculations for these and other bcc (001) systems. Such localized $\overline{\Gamma}$ surface states have mainly $d_{3z^2-r^2}$ symmetry with lobes pointing into the vacuum region and are a characteristic feature of bcc (001) surfaces. These states are Shockley-like surface states arising from the large hybridization (symmetry) gap formed between the two bulk Δ_1 bands, which are composed of s orbitals and $d_{3z^2-r^2}$ orbitals. (The other d orbitals belong to different representations and do not interact with these orbitals.) At both the bulk zone center and the H point (the end of the bulk Δ line), these orbitals do not mix, with the s (d) orbital belonging to the Γ_1 (Γ_{12}) irreducible representation, but the relative order of the s and d states at Γ and H is reversed. This symmetry required change in the s to d orbital character of each Δ_1 band between Γ and H holds for bulk states but not for surface states. This Shockley-like mechanism [20] gives rise to surface states in the gap, which have an evanescent decay into the crystal, as displayed in Fig. 4. In the absence of s-d hybridization, the $d_{3z^2-r^2}$ band would lie completely within this hybridization gap, and the resulting split-off state is thus mainly of $d_{3z^2-r^2}$ character.

As a further test of the generality of these surface states, we examined the tunneling spectra of the Cr(001) surface. Figure 5 shows the tunneling conductance spectra of the Cr(001) surface. A narrow peak, similar to the Fe(001) spectra in Fig. 1, is observed. This feature lies 0.05 eV below the Fermi level. A feature at this energy was previously seen in photoemission spectra from this surface, but it was interpreted as part of a broader exchange split peak above the Fermi level that was cut off at the Fermi edge [21] (photoemission measurements sample only filled states). The spectra in Fig. 5 show that this state is very narrow and located below the Fermi level.

Calculations for a 13-layer Cr(001) film also give a very localized surface state near the Fermi level. The

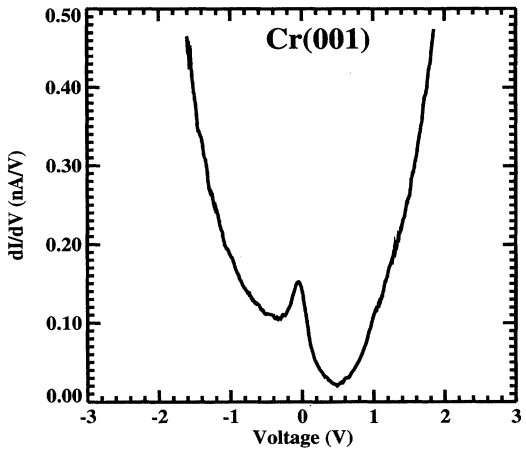

FIG. 5. Tunneling conductance vs sample voltage measurements of the Cr(001) surface obtained at constant height above the Fe surface. The tunneling conductance data were obtained from the numerical differentiation of the current vs voltage measurements using an energy window of 0.05 eV. The Cr(001) surface was obtained by growing six monolayers of Cr on an Fe(001) whisker at 270 °C.

positions of these peaks in the vacuum LDOS, however, are quite sensitive to the surface magnetic moment. The self-consistent local spin density calculations predict an enhanced surface moment of $2.5\mu_B$ at $T = 0$ K, compared to the measured (calculated) bulk moment of $0.59\mu_B$ ($0.62\mu_B$). A large surface state exchange splitting of around 1.7 eV results from the calculation and places the minority and majority peaks at 0.55 and -1.15 eV, respectively. For a paramagnetic calculation, on the other hand, there is a single peak at -0.22 eV. Note that the magnetism of Cr is quite complicated. The limitations in the local spin density approximation, coupled with the fact that the Néel temperature is only 311 K, suggest that it is not unlikely that the experimental surface moment may be reduced compared to the calculations. From a number of model calculations in which the surface moments (but not bulk moments) are artificially reduced, reasonable agreement with the experimental tunneling spectra (Fig. 5) is obtained for a surface moment of $1.75\mu_B$, which places the minority peak at -0.05 eV.

In summary, we have shown that a bcc surface state near the Fermi level can be observed in the tunneling spectra of Fe(001) and Cr(001) surfaces. Band-structure calculations show this state is a general characteristic of bcc (001) surfaces and originates from a nearly unperturbed d atomic orbital extending into the vacuum region. Use of this surface state will provide a means to achieve chemical identification with atomic spatial resolution in future studies, such as heteroepitaxial growth on bcc (001) surfaces. On magnetic bcc (001) surfaces the polarized nature of this surface state will benefit spin-polarized tunneling experiments.

We are grateful to W. Gadzuk, M. D. Stiles, and R. Wu for helpful discussions. This work was supported by the Office of Technology Administration of the Department of Commerce and the Office of Naval Research and the Division of Materials Sciences, U.S. Department of Energy, under Contract No. DE-AC02-76CH00016.

[1] G. Binnig and H. Rohrer, Helv. Phys. Acta **55**, 726 (1982).
[2] R. S. Becker, J. A. Golovchenko, D. R. Hamann, and B. S. Swartzentruber, Phys. Rev. Lett. **55**, 2032 (1985).
[3] R. J. Hamers, J. E. Demuth, and R. M. Tromp, Phys. Rev. Lett. **56**, 1972 (1986).
[4] *Scanning Tunneling Microscopy,* edited by J. A. Stroscio and W. J. Kaiser, Methods of Experimental Physics Vol. 27 (Academic, New York, 1993).
[5] J. A. Stroscio, R. M. Feenstra, and A. P. Fein, Phys. Rev. Lett. **57**, 2579 (1986).
[6] Y. Kuk, in *Scanning Tunneling Microscopy* (Ref. [4]), p. 284.
[7] T. Jung, Y. W. Mo, and F. J. Himpsel, Phys. Rev. Lett. **74**, 1641 (1995).
[8] M. Schmid, H. Stadler, and P. Varga, Phys. Rev. Lett. **70**, 1441 (1993).
[9] M. F. Crommie, C. P. Lutz, and D. M. Eigler, Nature (London) **363**, 524 (1993).
[10] Y. Hasegawa and Ph. Avouris, Phys. Rev. Lett. **71**, 1071 (1993).
[11] Ph. Avouris, I.-W. Lyo, R. E. Walkup, and Y. Hasegawa, J. Vac. Sci. Technol. B **12**, 1447 (1994).
[12] A. S. Arrott, B. Heinrich, and S. T. Purcell, in *Kinetics of Ordering and Growth at Surfaces,* edited by M. G. Lagally (Plenum, New York, 1990), p. 321.
[13] J. A. Stroscio, D. T. Pierce, and R. A. Dragoset, Phys. Rev. Lett. **70**, 3615 (1993); J. A. Stroscio and D. T. Pierce, J. Vac. Sci. Technol. B **12**, 1783 (1994).
[14] N. B. Brookes, A. Clarke, P. D. Johnson, and M. Weinert, Phys. Rev. B **41**, 2643 (1990).
[15] M. Weinert, E. Wimmer, and A. J. Freeman, Phys. Rev. B **26**, 4571 (1982).
[16] J. Tersoff and D. R. Hamann, Phys. Rev. Lett. **50**, 1998 (1983); Phys. Rev. B **31**, 805 (1985).
[17] E. W. Plummer and J. W. Gadzuk, Phys. Rev. Lett. **25**, 1493 (1970); J. W. Gadzuk and E. W. Plummer, Rev. Mod. Phys. **45**, 487 (1973).
[18] S. L. Weng, E. W. Plummer, and T. Gustafsson, Phys. Rev. B **18**, 1718 (1978).
[19] X. Pan, E. W. Plummer, and M. Weinert, Phys. Rev. B **42**, 5025 (1990).
[20] W. Shockley, Phys. Rev. **56**, 317 (1939).
[21] L. E. Klebanoff, R. H. Victora, L. M. Falicov, and D. A. Shirley, Phys. Rev. B **32**, 1997 (1985).